physica status solidi b
www.pss-b.com
basic solid state physics

The role of environmental effects on the optical transition energies and radial breathing mode frequency of single wall carbon nanotubes

P. T. Araujo[1] and A. Jorio[1,2]

[1] Departamento de Física, Universidade Federal de Minas Gerais, Belo Horizonte, MG, 30123-970, Brazil
[2] Divisão de Metrologia de Materiais, Instituto Nacional de Metrologia, Normalização e Qualidade Industrial (Inmetro), Duque de Caxias, RJ, 25250-020, Brazil

Received 30 April 2008, revised 23 June 2008, accepted 24 June 2006
Published online 29 August 2008

PACS 63.22.Gh, 78.30.Na, 78.67.Ch

In this paper we discuss the environmental effects on the radial breathing mode (RBM) spectra of Single Wall Carbon Nanotubes (SWNTs). We have shown that the environmental effect on the radial breathing mode frequencies can be explained by Van-der-Waals interactions. We here explore these interactions concerning its (n, m) dependence and curvature effects. Furthermore, most of the optical transition energies available in the literature ($E_{ii}^{\mathrm{Lit.}}$) are downshifted with respect to the optical transition energies for super-growth (S.G.) tubes ($E_{ii}^{\mathrm{S.G.}}$). The effect on transition energies can be understood considering the effect of the dielectric constant of the medium in the excitonic optical transition.

phys. stat. sol. (b) **245**, No. 10, 2201–2204 (2008) / **DOI** 10.1002/pssb.200879625

phys. stat. sol. (b) **245**, No. 10, 2201–2204 (2008) / **DOI** 10.1002/pssb.200879625

physica status solidi b
www.pss-b.com
basic solid state physics

The role of environmental effects on the optical transition energies and radial breathing mode frequency of single wall carbon nanotubes

P. T. Araujo[1,*] and A. Jorio[1,2]

[1] Departamento de Física, Universidade Federal de Minas Gerais, Belo Horizonte, MG, 30123-970, Brazil
[2] Divisão de Metrologia de Materiais, Instituto Nacional de Metrologia, Normalização e Qualidade Industrial (Inmetro), Duque de Caxias, RJ, 25250-020, Brazil

Received 30 April 2008, revised 23 June 2008, accepted 24 June 2006
Published online 29 August 2008

PACS 63.22.Gh, 78.30.Na, 78.67.Ch

* Corresponding author: e-mail pauloata@fisica.ufmg.br, Phone: +55-31-34096610, Fax: +55-31-34095600

In this paper we discuss the environmental effects on the radial breathing mode (RBM) spectra of Single Wall Carbon Nanotubes (SWNTs). We have shown that the environmental effect on the radial breathing mode frequencies can be explained by Van-der-Waals interactions. We here explore these interactions concerning its (n, m) dependence and curvature effects. Furthermore, most of the optical transition energies available in the literature ($E_{ii}^{\mathrm{Lit.}}$) are downshifted with respect to the optical transition energies for super-growth (S.G.) tubes ($E_{ii}^{\mathrm{S.G.}}$). The effect on transition energies can be understood considering the effect of the dielectric constant of the medium in the excitonic optical transition.

1 Introduction The effects of different kinds of environments on the properties of single wall carbon nanotubes (SWNTs) have been extensively discussed [1]. Most of the difficulties are directly related to the absence of a reference material, establishing the standard properties. In this work we have studied, using resonance Raman spectroscopy, a sample composed by super-growth (S.G.) SWNTs that seems to fulfill such reference requirement. First, the S.G. optical transitions energies ($E_{ii}^{\mathrm{S.G.}}$) are upshifted from all the data available in the literature [2–15]. Since the dielectric constant (ε) of the environment decreases E_{ii}, this result indicates the S.G. SWNTs represent a system with smallest ε, *i.e.* $\varepsilon \rightarrow 1$ [16]. Second, the radial breathing mode frequencies for specific (n, m) SWNTs measured in the S.G. sample ($\omega_{\mathrm{RBM}}^{\mathrm{S.G.}}$) are redshifted from all the results published in the literature [2–11]. Since tube interaction is expected to increase ω_{RBM}, this result also indicates the S.G. SWNTs exhibit the weakest interaction with the environment. Furthermore, recently it was shown that the relation $\omega_{\mathrm{RBM}} = A/d_t + B$ between the $\omega_{\mathrm{RBM}}^{\mathrm{S.G.}}$ and tube diameter (d_t) follows the equation $\omega_{\mathrm{RBM}}^{\mathrm{S.G.}} = 227/d_t$, which is in perfect agreement with the elastic property of graphite and with a negligible environmental effect ($\mathbf{B} \approx \mathbf{0}$) [18]. By comparing $\omega_{\mathrm{RBM}}^{\mathrm{S.G.}}$ with other ω_{RBM} values reported in the literature, coming from SWNTs surrounded by different types of environments, it was shown that the non-null $\mathbf{B}$ constant can be modeled considering the Van-der-Waals interactions between the SWNTs walls and the surrounding material [17, 18]. Here, we discuss the $E_{ii}^{\mathrm{S.G.}}$ and we point to several details about the Van-der-Waals potential mediating the interaction between SWNTs and their environment.

2 Experimental details The sample we have used was synthesized using a special water-assisted CVD process, baptized "super-growth" process, generating millimeter-long and high-purity SWNTs. Besides the length, the "super-growth" SWNTs exhibit a broad diame-

ter distribution (d_t from 1 to 4 nm) and all tube chiralities ($0^\circ \leq \theta \leq 30^\circ$). The tubes are vertically aligned from a silicon substrate to form a very sparse material, where SWNTs represent only 3.6% of the total volume [19–22].

To determine both the optical transition energies E_{ii} and the radial breathing mode frequencies $\omega_{\rm RBM}$ of each SWNT type, we have used the resonance Raman scattering technique with a tuneable laser excitation. Two triple-monochromator Raman spectrometers, equipped with coupled charge device (CCD) detectors, were used in the back-scattering configuration to perform the measurements - a Dilor XY for experiments in the visible range and a SPEX in the near infrared range. We used a total of 125 different excitation laser energies (ArKr, Ti:Sapphire and Dye lasers) from 1.26 eV to 2.71 eV. The light reaches the sample from the top and the laser power density at the sample is maintained constant and low enough not to produce heating effects (1 mW focused with an 80× objective in the visible, and 25 mW focused with a 10 cm focal distance length in the infrared). A tungsten halogen lamp and 4-Acetamidophenol (tylenol) are used for calibration in the visible and infrared, respectively.

3 Optical transition energy analysis The radial breathing mode region of each Raman spectra is composed by a convolution of several Lorentizians, each Lorentizian representing a different SWNT specie which is in resonance with the laser energy. Due to the broad energy range, we measured 125 Raman spectra with different excitation laser energies. By fitting each of the spectra with Lorentizians we have clearly assigned the (n, m) indices of 197 different SWNT. The resonance profiles for the other (n, m) tubes in this range overlap to each other and no clear assignment was possible. This method of assignment is extensively discussed in the literature [9,11,23]. Figure 1 shows a general view of the experiment.

In Fig. 1(a) the 125 resonance Raman spectra were used to generate a two-dimensional plot giving the Raman intensity as a function of the laser excitation energy (E_{laser}) and radial breathing mode frequency ($\omega_{\rm RBM}$). A Raman peak appears at a given $\omega_{\rm RBM}$ whenever E_{laser} reaches the optical transition energy (E_{ii}), i.e. when resonance is established for a given carbon nanotube in the sample. Figure 1(b) is a plot of all $E_{ii}^{\rm S.G.}$ as a function of $\omega_{\rm RBM}^{\rm S.G.}$. $E_{ii}^{\rm S.G.}$ is ranging from $E_{11}^{\rm S}$ up to $E_{66}^{\rm S}$ (here S stands for semiconducting tube, otherwise M will be used for metallic tubes). Figure 1(c) gives the Kataura plot for SWNTs. All the $\omega_{\rm RBM}$ values were obtained using the relation $\omega_{\rm RBM} = 227/d_t$ [18] and the E_{ii} values were obtained by fitting the $E_{ii}^{\rm S.G.}$ in Fig. 1 using the equation [11]:

$$E_{ii}(p, d_t) = 1.074\frac{p}{d_t}\left[1 + 0.467\log\frac{0.812}{p/d_t}\right] + \beta_p \cos 3\theta/d_t^2\,, \quad (1)$$

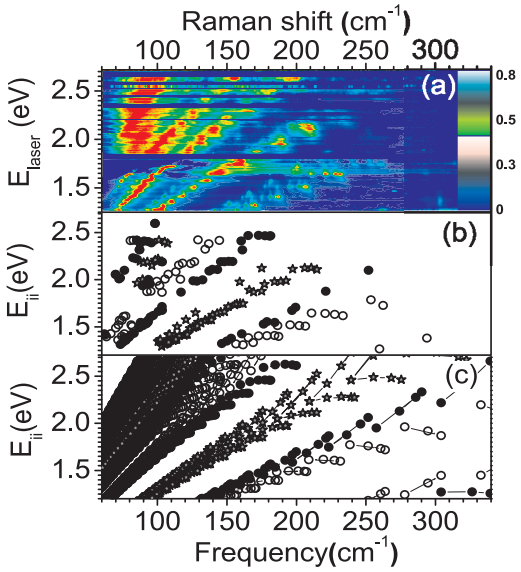

Figure 1 (color online) (a) 2D color map showing the S.G. SWNT RBM spectral evolution as a function of excitation laser energy. The intensity of each spectrum is normalized to the strongest peak. (b) Plot of all transitions energies ($E_{ii}^{\rm S.G.}$) experimentally obtained as a function of $\omega_{\rm RBM}$. (c) The Kataura plot for S.G. SWNTs. The transition energies were calculated using Eq. (1), that is obtained by fitting the available $E_{ii}^{\rm S.G.}$ (panel (b)) and plotted as a function of $\omega_{\rm RBM}$, given by $\omega_{\rm RBM} = 227/d_t$ [18]. In (b) and (c) the gray stars stand for metallic tubes, the black bullets stand for type I semiconducting tubes and the opened bullets stand for type II semiconducting tubes.

where p is defined as $1, 2, 3, ..., 8$ for $E_{11}^{\rm S}$, $E_{22}^{\rm S}$, $E_{11}^{\rm M}$,...,$E_{66}^{\rm S}$, respectively. The β_p values for the lower(upper) E_{ii} branches are -0.07(0.09), -0.18(0.14), -0.19(0.29), -0.33(0.49), -0.43(0.59), -0.6(0.57), -0.6(0.73) and -0.65(?) for $p = 1, 2, 3, ..., 8$, respectively. To calculate E_{ii} higher than $E_{11}^{\rm M}$ ($p > 3$) the term $0.059p/d_t$ has to be added to the Eq. (1). A detailed discussion about equation 1 is found in references [11,23].

In order to understand the effect of the environment on $E_{ii}^{\rm S.G.}$ we have compared our results with others available in the literature. Figure 2 shows the difference between E_{ii} from the literature ($E_{ii}^{\rm Lit.}$) and $E_{ii}^{\rm S.G.}$ as a function of tube diameter. The energy difference ($\Delta E_{ii} = E_{ii}^{\rm Lit.} - E_{ii}^{\rm S.G.}$) has an average dependence on d_t (see black solid curve in Fig. 2). We tried to separate the information according to chiral angle (see the inset in Fig. 2), $2n + m$ families, the SWNTs type and E_{ii} transition levels, but no specific trends could be observed .

In Fig. 2, except for the star symbols that come from Rayleigh scattering [15], all the other ΔE_{ii} are negative, *i.e.* the E_{ii} values for the water-growth assisted sample measured here are higher than all the values published in the literature. This result suggests we measured the optical

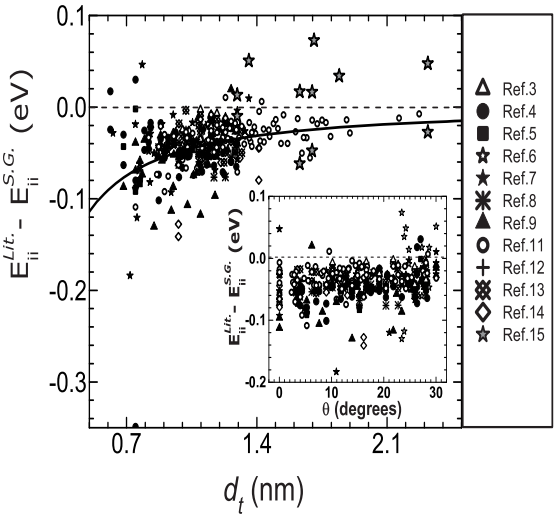

Figure 2 The difference between E_{ii} obtained from the literature ($E_{ii}^{\mathrm{Lit.}}$) and E_{ii} from this work ($E_{ii}^{\mathrm{S.G.}}$) are plotted as a function of d_t. Each symbol represents data from a different reference (see legend). The black solid line is a guide to the eye for the average value of ΔE_{ii}. The inset shows ΔE_{ii} as a function of chiral angle (θ). No dependence with chiral angle or $2n + m$ families are observed.

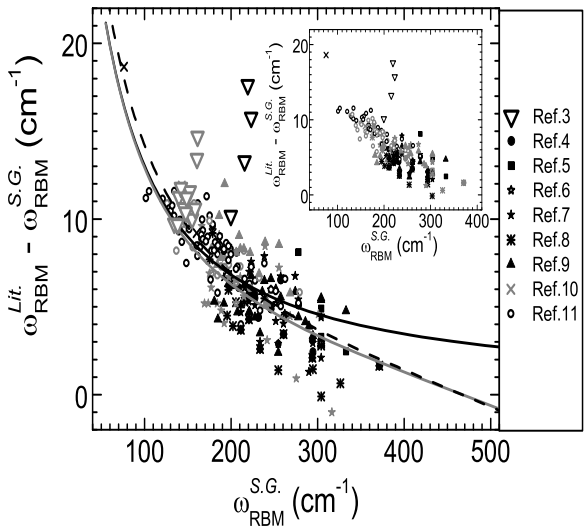

Figure 3 Difference between ω_{RBM} data from the literature ($\omega_{\mathrm{RBM}}^{\mathrm{Lit.}}$) and ω_{RBM} data from this work ($\omega_{\mathrm{RBM}}^{\mathrm{S.G.}}$) as a function of $\omega_{\mathrm{RBM}}^{S.G}$. Each symbol represents data from a different reference (see legends). The black solid line is a fit to the data using the Eq. (2). The gray and the dashed lines are, respectively, the fit considering only curvature effects and curvature effects plus pressure contributions [27]. The black symbols stand for semiconducting tubes and the gray symbols stand for metallic tubes. The inset brings the same plot but now the black symbols stand for type I semiconducting tubes and the gray symbols stand for type II tubes.

properties of pristine SWNTs in a dielectric constant environment of $\varepsilon \rightarrow 1$. As predicted by Miyauchi *et al.* [24], an increase of the dielectric constant of the environment generates a downshift in E_{ii}. The usually obtained results ($\varepsilon = 2.2$) generates a downshift of about ~ 40 meV, that should depend on d_t, exactly as observed in our experiment.

4 The Van-der-Waals potential mediates the interaction between SWNT and their environment

A lot of efforts have been made to understand the environment effects on ω_{RBM}. Recently, we showed that the Van-der-Waals potential mediates the interaction between SWNTs and their environment [18]. The relation between $\omega_{\mathrm{RBM}}^{\mathrm{S.G.}}$ and d_t was found to be $\omega_{\mathrm{RBM}}^{\mathrm{S.G.}} = 227/d_t$, which is accordance with the elastic property of graphite [25, 26]. The difference between $\omega_{\mathrm{RBM}}^{\mathrm{Lit.}}$ and $\omega_{\mathrm{RBM}}^{\mathrm{S.G.}}$ ($\Delta\omega_{\mathrm{RBM}} = \omega_{\mathrm{RBM}}^{\mathrm{Lit.}} - \omega_{\mathrm{RBM}}^{\mathrm{S.G.}}$) is a diameter dependent relation given by:

$$\Delta\omega_{\mathrm{RBM}} = 227.0 \left(\frac{1}{d_t} - \left[\frac{1}{d_t^2} + \frac{6(1-\nu^2)}{Eh} \frac{K}{s_0^2} \right]^{1/2} \right), \quad (2)$$

where [6(1 - ν^2)/Eh] = 26.3 Å^2/eV and K/s_0^2 is an adjustable parameter [18,27].

Figure 3 shows $\Delta\omega_{\mathrm{RBM}}$ plotted as a function of $\omega_{\mathrm{RBM}}^{\mathrm{S.G.}}$. The black solid line is a fitting proposed in [18] using Eq. (2) with $K/s_0^2 = (2.2 \pm 0.1)$ meV/Å^4. The Van-der-Waals interactions happen between the SWNT π orbital and π or σ orbital of the environment system [28]. Therefore it is reasonable to wonder if it makes sense to consider curvature effects or even pressure on the tube wall due to environment surrounding. Curvature effects are expected to influence the system only for small diameters tubes ($d_t < 1.2$ nm), where re-hybridization of the π and σ orbital in the SWNT structure is significant. Such re-hybridization can change both the interaction strength of the Van-der-Waals potential and the tube C-C bound strength [28–30]. To account for the curvature effects, we have included in Eq. (2) an extra term equals to A/d_t^2, as a first approximation. After fitting the data, the constant A was found equals to $0.7 \pm 0.2\, nm^2$ and the result is the gray solid line in Fig. 3, showing us an improvement compared to the result coming from the Eq. (2). Furthermore, the hydrostatic pressure on the tube wall is expected to change ω_{RBM} by about 10% of $\Delta\omega_{\mathrm{RBM}}$ [29]. The result of the fitting including both curvature and pressure effects is shown in Fig. 3 by the dashed curve. The improvement is negligible considering

the data spread in larger diameter tubes ($d_t > 1.2$ nm), but for smaller diameter tubes, $\sigma - \pi$ hybridization plays a role in the tube-environment interaction. These results demonstrate that the Eq. (2)) is enough to describe our results.

No difference in $\Delta\omega_{\mathrm{RBM}}$ could be observed between metallic and semiconducting nanotubes interactions with the environment, as evidenced by the black and gray symbols in Fig. 3 (the black symbols stand for semiconducting tubes and gray symbols stand for metallic tubes). Theoretically, such a difference could exist because of the free electrons present in the electronic structure of metallic tubes [30]. The inset in Fig. 3 also shows that no difference could be observed between type I and II semiconducting tubes (the black symbols stand for type I and the gray stand for type II).

5 Conclusions In this work we study the role of the environment in the Raman spectra of SWNTs. We compare the optical transition energies obtained from "super-growth" SWNTs with others in the literature, showing that all the transition energies for the "super-growth" SWNTs are upshifted by about 40 meV from the values in the literature, suggesting that the "super-growth" SWNTs are surrounded by vacuum. The difference between $E_{ii}^{\mathrm{Lit.}}$ and $E_{ii}^{\mathrm{S.G.}}$ shows some dependence with tube diameter, but no chirality dependence was observed. The interaction between SWNTs and their environment is mediated by the Van-der-Waals potential [18]. Because of the nature of the interactions, curvature effects could be important. Here we show an improvement on fitting the data considering a $1/d_t^2$ dependence that occurs for higher frequency RBMs ω_{RBM} *i.e.* for smaller diameter tubes ($d_t < 1.2$ nm. The pressure due the environment on the SWNT wall does not significantly contribute to the ω_{RBM} changes.

Acknowledgements The authors acknowledge CNPq, CAPES and Fapemig for financial support.

References

[1] A. Jorio, M. S. Dresselhaus and G. Dresselhaus, Carbon Nanotubes: Advanced Topics in Synthesis, Properties and Applications, Top. Appl. Phys., Vol. 111 (Springer, Berlin, 2007).
[2] M. Milnera et al., Phys. Rev. Lett. **84**, 1324 (2000).
[3] A. Jorio et al., Phys. Rev. Lett. **86**, 1118 (2001).
[4] S. M. Bachilo et al., Science **298**, 2361 (2002).
[5] A. Hartschuh et al., Science **301**, 1354 (2003).
[6] M. Strano et al., Nano Lett. **3**, 1091 (2003).
[7] H. Telg et al., Phys. Rev. Lett. **93**, 177401 (2004).
[8] S. K. Doorn et al., Appl. Phys. A **78**, 1147 (2004).
[9] C. Fantini et al., Phys. Rev. Lett. **93**, 147406 (2004).
[10] M. Paillet et al., Phys. Rev. Lett. **96**, 257401 (2006).
[11] P. T. Araujo et al., Phys. Rev. Lett. **98**, 067401 (2007).
[12] J. Lefebvre et al., Appl. Phys. A **78**, 1107 (2004).
[13] Y. Ohno et al., Phys. Rev. B **73**, 235427 (2006).
[14] H. Son et al., Phys. Rev. B **74**, 073406 (2006).
[15] M. Y. Sfeir et al., Science **312**, 554 (2006).
[16] A. G. Walsh et al., Nano Lett. **7**, 1485 (2007).
[17] C. Thomsen et al., phys. stat. sol. (b) **215**, 435 (1999).
[18] P. T. Araujo, Phys. Rev. B, rapid communications (2008), in press.
[19] K. Hata, Science **306**, 1362 (2004).
[20] D. N. Futaba, Phys. Rev. Lett. **95**, 056104 (2005).
[21] D. N. Futaba, J. Phys. Chem. B **110**(15), 8035 (2006).
[22] D. N. Futaba, Nature Mater. **5**, 987 (2006).
[23] A. Jorio, phys. stat. sol. (b) **244**, 4011 (2007).
[24] Y. Miyauchi, arXiv:0704.1380v1 [cond-mat.mtrl-sci] 11 apr 2007.
[25] G. D. Mahan, Phys. Rev. B **65**, 235402 (2002).
[26] V. N. Popov and P. Lambin, Phys. Rev. B **73**, 085407 (2006).
[27] M. J. Longhurst and N. Quirke, J. Chem. Phys. **124**, 234708 (2006).
[28] L. A. Girifalco, Phys. Rev. B **62**, 13104 (2000).
[29] U. D. Venkateswaran, Phys. Rev. B **68**, 241406(R) (2003).
[30] M. J. Longhurst and N. Quirke, Phys. Rev. Lett. **98**, 145503 (2007).

